Available online at www.sciencedirect.com
SCIENCE DIRECT®
Journal of Magnetic Resonance 176 (2005) 99–106
JMR Journal of Magnetic Resonance
www.elsevier.com/locate/jmr

Communication

DENSE with SENSE

Anthony H. Aletras *, W. Patricia Ingkanisorn, Christine Mancini, Andrew E. Arai

Laboratory of Cardiac Energetics, National Heart, Lung and Blood Institute, National Institutes of Health, Department of Health and Human Services, Bethesda, MD, USA
Suburban Hospital Healthcare System, Bethesda, MD, USA

Received 27 September 2004; revised 3 May 2005
Available online 8 June 2005

Abstract

Displacement encoding with stimulated echoes (DENSE) with a low encoding strength phase-cycled meta-DENSE readout and a two fold SENSE acceleration ($R = 2$) is described. This combination reduces total breath-hold times for increased patient comfort during cardiac regional myocardial contractility studies. Images from phantoms, normal volunteers, and a patient are provided to demonstrate the SENSE–DENSE combination of methods. The overall breath-hold time is halved while preserving strain map quality.
Published by Elsevier Inc.

Keywords: Myocardial; Contraction; Cardiac; Function; SPAMM; DENSE; HARP; Tagging; Heart; MRI; Strain

1. Introduction

Displacement encoding with stimulated echoes (DENSE) can map regional myocardial strain [1] as an alternative to existing myocardial tagging methods [2,3]. Regional circumferential shortening (CS) and radial thickening (RT) strain measurements can be obtained. The complex DENSE data acquisition method has been introduced [4] and recently applied [5,6] for imaging strain in humans [1,7–9]. In short, complex data acquisition relies on two 90° phase-cycled acquisitions to sample both the real and imaginary components of the stimulated echo acquisition mode (STEAM) [10] signal so that the entire complex magnetization vector can be reconstructed in order to suppress the stimulated anti-echo [11]. Due to the lower gradient first-order moments required for displacement encoding, the complex acquisition results in reduced intravoxel dephasing artifacts [5] while also suppressing myocardial tag-like artifacts, which originate from the stimulated anti-echo. Additional tag-like artifacts that originate from the T_1-recovering signal (a.k.a. FID, DC) are also suppressed so that quality DENSE data can be obtained [5,6]. This FID suppression is performed either with additional phase-cycling [6] or with an inversion pulse [5], which is strategically placed within the motion encoding interval of a mixed echo-train acquisition DENSE (meta-DENSE) [8] experiment, which is based on a train of refocusing pulses for acquiring multiple k-space lines per excitation.

When compared to the original non-complex acquisition DENSE technique [1], which exhibits intravoxel dephasing artifacts, these new phase-cycling schemes improve image quality at the cost of prolonging the data acquisition so that it cannot be completed within the limits of a reasonable breath-hold. With meta-DENSE, the use of the complex acquisition increased the scan time from 14 [8] to 20 [5] heartbeats. The former is a reasonable breath-hold time for patients while the latter can only be used consistently in normal volunteers. This increased scan time was present despite attempts to speed up the data acquisition process by increasing the echo-train length (ETL) in the complex acquisition (from 24 to 32), which degrades the

* Corresponding author. Fax: +1 301 402 2389
E-mail address: AletrasA@nhlbi.nih.gov (A.H. Aletras).

1090-7807/$ - see front matter. Published by Elsevier Inc.
doi:10.1016/j.jmr.2005.05.010

point spread function and introduces motion blurring due to the longer acquisition window.

Parallel imaging has been introduced as a method for accelerating MR image acquisition by under-sampling the phase encoding direction and taking into account the inherent spatial information of multiple receiver coils [12]. Different methodologies have been applied either in k-space [13,14] or on the images themselves [15,16] so as to incorporate surface coil array signals into the reconstruction process and resolve the aliasing that results from under-sampling. With SENSE [15], a filter is applied by mapping the spatial sensitivities of the phased array elements used to receive the signals. The premise is that these sensitivities have slow-varying spatial characteristics and that they can be mapped via a low resolution image. Also, to account for coupling between the array's coil elements, a noise-only acquisition is used to calculate individual coil gains and cross-correlation. To date, parallel imaging acceleration has not been implemented for mapping cardiac motion and function with phase contrast methods such as DENSE. The main concern is the signal-to-noise penalty imposed by parallel imaging to DENSE, which is based on stimulated echoes where 50% of the signal is lost. Especially since the computations to extract regional strain values are inherently noisy, this concern becomes paramount for mapping regional function.

We present mixed echo-train acquisition displacement encoding with stimulated echoes (meta-DENSE) myocardial strain imaging with SENSE acceleration. This is the first implementation of SENSE with a phase contrast method to map cardiac motion. Images from phantoms, normal volunteers, and patients are presented. The implemented SENSE acceleration factor of 2 allows for 2D strain imaging within 14 heartbeats thus making the method appropriate for clinical use. Quantification of the noise in these measurements is also presented.

2. Methods

An eight receiver General Electric Medical Systems (Waukesha, WI) 1.5 T Excite (version 10.0) magnet was used for all experiments. A four coil cardiac phased array (General Electric Medical Systems, Waukesha, WI) was used for static phantom experiments while an eight coil phased array (Nova Medical, Boston, MA) was used for rotating phantom and human experiments. The phantom consisted of a $CuSO_4$ doped agarose cylindrical container ($T_1 = 825$ ms) to simulate the myocardium and one rectangular container with a shorter T_1 (130 ms) to simulate fat in the chest wall. The cylindrical "myocardial" phantom could be rotated along its long axis at 0.5 Hz. Imaging parameters similar to those used for normal volunteer experiments, as described below, were used.

DENSE images were acquired from normal volunteers and a patient with a chronic myocardial infarction both with full k-space sampling and with SENSE acceleration ($R = 2$). Position encoding of spins was triggered on the R-wave of the ECG [1,7,8] at 4.0 mm/π and image acquisition occurred at end-systole along the short axis slice of the heart. The encoding interval (approximately 300 ms) was determined by finding the trigger delay to end systole on a long axis cine MRI scan. During this interval, a Silver–Hoult adiabatic inversion pulse was applied to suppress the FID as previously described [8]. The ETL was 24 for a readout period of 118 ms/heartbeat. The matrix size was 128×96 with a rectangular field of view (FOV) resulting in $2.9 \times 2.9\ \text{mm}^2$ in-plane resolution which was linearly interpolated to 10 times its original size for viewing the strain maps within a 52×52 submatrix centered around the left ventricle. Manual segmentation, on the magnitude images, of the endocardial and epicardial borders was performed for strain display purposes. Other parameters were: slice thickness 8 mm, bandwidth ±62.5 kHz, TE 3 ms, TR of 1 RR interval.

For 2D displacement mapping and strain processing, X-encoded, Y-encoded, and a phase reference scan were acquired at the same spatial resolution. Therefore, a typical 2D acquisition can be described as X/Y/REF. The phase reference scan REF was used for increasing the signal-to-noise ratio and for correcting for local B_0 inhomogeneity by subtraction from the encoded scans as previously described [1]. In brief, the DENSE gradient displacement encoding moments (k_X and k_Y) along the two in-plane directions were halved and their sign was toggled between the reference scan and the each of the encoded directions. As such, the three scans were executed with the following gradient moments along the corresponding axes: REF with $-k_X/2$ and $-k_Y/2$; X with $+k_X/2$ and $-k_Y/2$; and Y with $-k_X/2$ and $+k_Y/2$. With RF-cycling to suppress the anti-echo, for non-accelerated complex meta-DENSE scans, a total of $(96/24) \times 3 \times 2 + 2 = 26$ heartbeats were needed per slice given the additional two discarded acquisitions that were used to set up the steady state. For RF-cycled SENSE-accelerated ($R = 2$) scans, a total of $(96/24/R) \times 3 \times 2 + 2 = 14$ heartbeats were required for each slice. In this case, the one discarded acquisition was instead used to collect a low resolution (128×24 matrix) full field of view fast-spin-echo (FSE) image for mapping the B_1 field of the phased array elements. For calculating the SENSE noise covariance matrix, an extra heartbeat prior to starting the breath-hold was dedicated to acquiring a noise-only dataset with the RF amplifier disabled.

For characterizing the in vivo strain noise, instead of acquiring REF/X/Y, the same gradient waveforms were applied so as to acquire REF/REF/REF, X/X/X and, Y/Y/Y datasets [8]. In this manner, ideally, the phase

recorded in the myocardium would be zero for all such datasets and also the computed strain would be zero. Any deviation from zero would be attributed to random or systematic noise sources. Strain values reported are rounded to the first decimal point.

Image reconstruction was performed with in-house software written in IDL (Research Systems, Boulder, CO). For accelerated scans, SENSE reconstruction was first performed for the X-encoded, Y-encoded, and reference half-FOV complex images. Tissue contrast was removed from the single heartbeat FSE images by dividing the image of each individual coil by the root sum of squares of images from all eight coils [15,16]. The resulting contrast-less FSE images had no motion encoding and were used for unaliasing the X, Y, and REF DENSE images by forming the sensitivity matrix S, as described by Pruessmann et al. [15]. The noise covariance matrix was computed from $24 \times 128 = 3072$ complex samples acquired during the noise-only scan. Following SENSE unaliasing [17], image processing proceeded as previously described [1] for calculating regional contractile strain. In brief, for every four pixels which formed a square within the myocardium the deformation was dissociated into a rotational component and two principle strain directions via eigenvector and eigenvalue analysis [18]. Eigenvectors with corresponding eigenvalues less than 1.0 were projected along the circumferential axis to yield circumferential shortening maps. The remaining eigenvectors were projected along the radial direction to yield radial thickening maps. Results are reported as mean ± standard deviation. Phase noise is reported in terms of its standard deviation since a non-spatially varying phase error will not propagate into the strain calculations due to the inherent spatial differentiation of strain calculations.

3. Results

Fig. 1 shows that undersampling the phase direction by a factor of 2 without the application of a SENSE filter results in half-FOV aliasing (top row) as seen in both magnitude and phase displacement images of a static phantom. Note that the "fat" ($T_1 = 130$ ms) rectangular phantom overlaps with the "myocardium" ($T_1 = 825$ ms) cylindrical phantom. With the SENSE filter applied (middle row) these aliasing artifacts are removed and the two phantoms are properly resolved in space. The SENSE-ac-

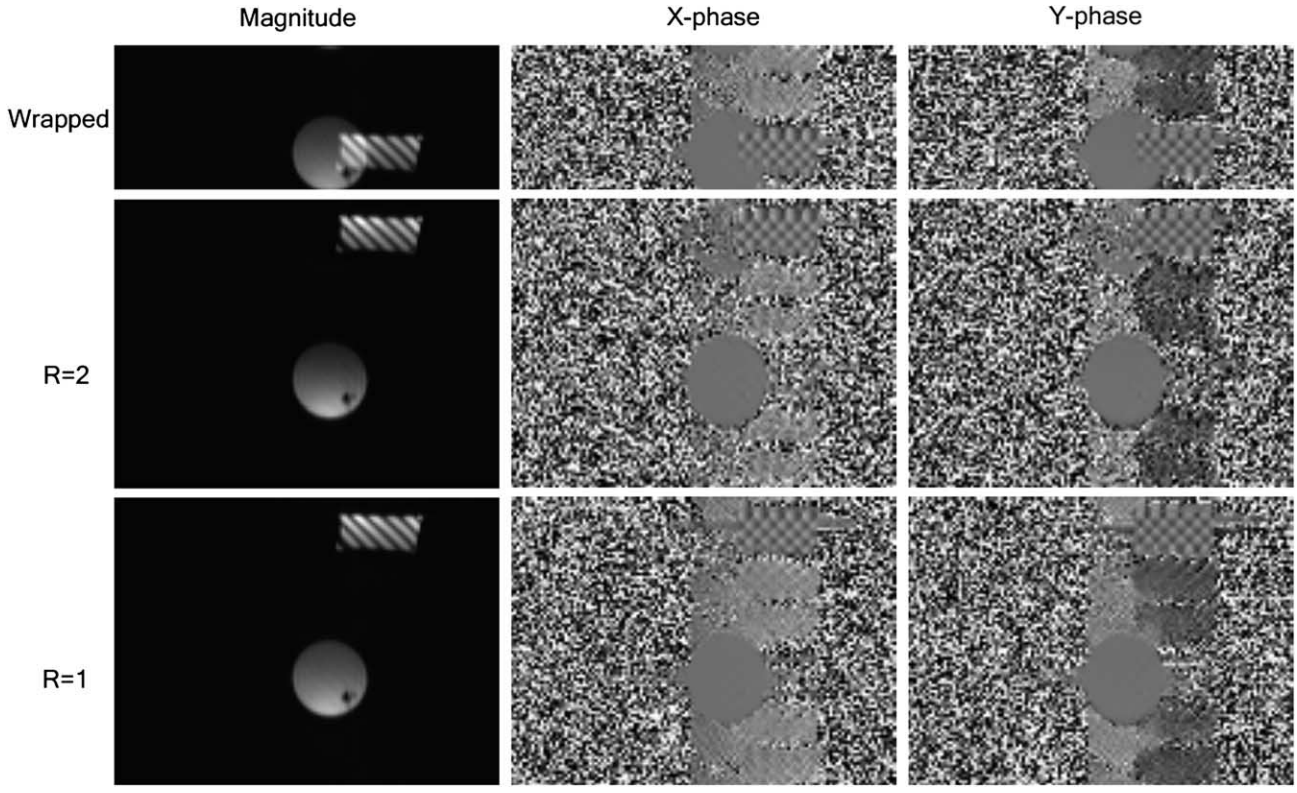

Fig. 1. SENSE-accelerated DENSE imaging results in reduced acquisition time (14 s) when compared to non-accelerated DENSE (26 s acquisition time) in stationary phantom data. The first row shows SENSE ($R = 2$) magnitude along with X and Y phase displacement phase data prior to applying the SENSE filter. Note the overlapping fat (rectangular, $T_1 = 130$ ms) and myocardial (cylindrical, $T_1 = 825$ ms) phantoms. The application of the SENSE filter (second row) unwraps the images. For $R = 2$ SENSE, the standard deviation of the phase measured in the "myocardium" was 0.087° for X and 0.088° for Y. Non-accelerated data with otherwise the same parameters are shown at the bottom row for reference. In this case, the standard deviation was 0.039° for X and 0.042° for Y. For computed strain noise in the phantom, see Section 3.

celerated DENSE images were acquired at half the time when compared to conventional non-accelerated ($R = 1$, bottom row) images. Note that, for both R values, tag-like artifacts are suppressed in the "myocardium" as a result of the encoding interval inversion pulse and the complex DENSE acquisition. Tag-like artifacts in the "fat" phantom are present because the inversion pulse is optimized for the T_1 of myocardium, not fat.

The measured phase noise in the static phantom (in terms of its standard deviation) represents the best case scenario of what can be expected in human scans with SENSE (0.087° for X and 0.088° for Y) and without SENSE (0.039° for X and 0.042° for Y). For human imaging one would expect other factors, such as motion, patient body size, variable coil loading, etc., to further increase the noise. The corresponding computed percent strain noise (images not shown) from these static phantom phase measurements also represents the best case scenario in terms of strain quantification with SENSE (0.3 ± 1.1 for CS and -0.2 ± 0.9 for RT) and without SENSE (0.2 ± 1.0 for CS and -0.1 ± 0.6 for RT). Rotating phantom experiments with SENSE (0.144° for X, 0.153° for Y, 0 ± 0.3 for CS, and 0 ± 0.3 for RT) and without SENSE (0.114° for X, 0.077° for Y, 0 ± 0.2 for CS, and 0 ± 0.3 for RT) showed similar trends.

Normal volunteer circumferential shortening (CS) and radial thickening (RT) maps of the left ventricle are shown in Fig. 2. Magnitude images are also shown for reference. The SENSE-accelerated (top row, 14 heartbeats) maps yielded average strains of 20.9 ± 8.0 for CS and 23.2 ± 9.1 for RT. The non-accelerated maps (bottom row, 26 heartbeats) yielded average strains of 21.2 ± 8.4 for CS and 23.9 ± 8.2 for RT. Note that qualitatively the two rows of data look similar despite the twofold acceleration.

Fig. 3 shows in vivo DENSE strain noise maps from a normal volunteer with SENSE acceleration factor $R = 2$. The rows show the acquisitions where all three encoding experiments were performed with the gradient waveforms of the reference scan (REF/REF/REF, top) or with those of the X-encoded scan (X/X/X, middle) or, last, those of the Y-encoded scan (Y/Y/Y, bottom). The noise measurements in terms of percent strain for all eight normal volunteers are summarized in Table 1. The noise is less than ±4.3% strain.

An example of SENSE acceleration from a patient with a chronic infarct who was capable of holding his breath for 26 heartbeats is shown in Fig. 4. In the figure inset, the gadolinium delayed enhanced image demonstrates the extent of the inferior myocardial infarct in

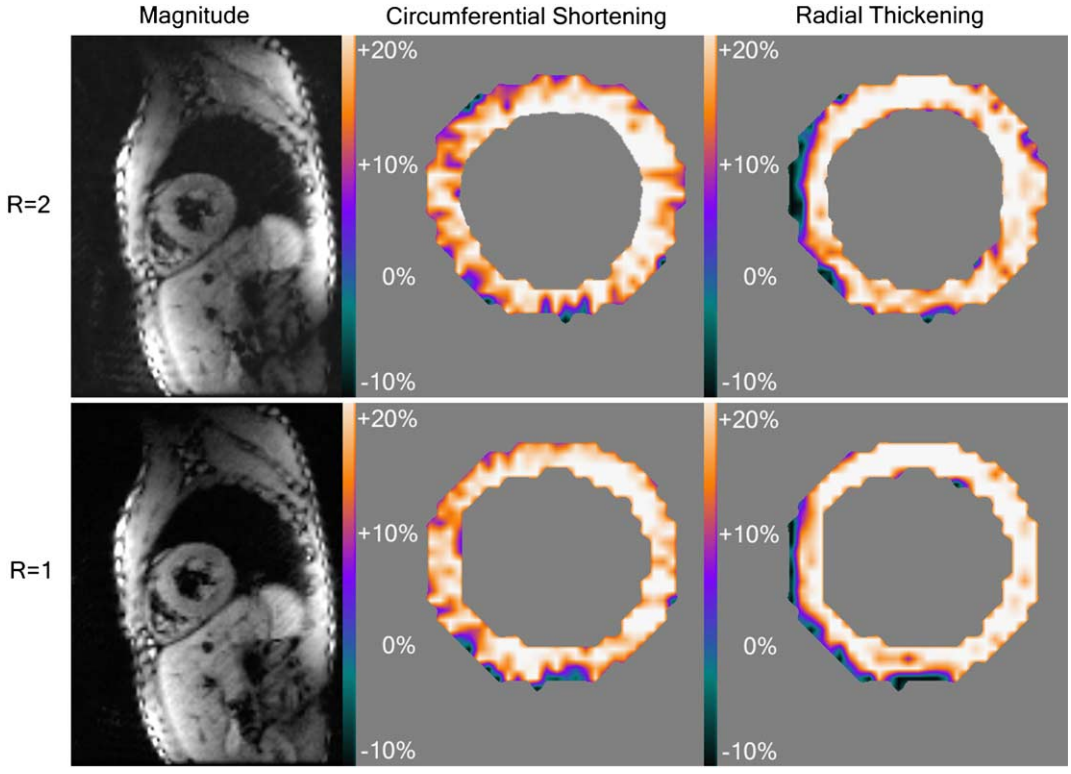

Fig. 2. Normal volunteer data demonstrate similar strain data with ($R = 2$, top row) and without ($R = 1$, bottom row) SENSE. The SENSE-accelerated data were acquired in 14 heartbeats in contrast to the non-accelerated dataset that was acquired in 26 heartbeats. The circumferential shortening measured in the heart was 20.9 ± 8.0 with SENSE and 21.2 ± 8.4 without SENSE. Corresponding values for radial thickening were 23.2 ± 9.1 and 23.9 ± 8.2 percent strain, respectively. The papillary muscles were manually cropped in left ventricular strain maps to avoid artificial measurements being created between them and the LV wall. Manual cropping also explains the differences observed in myocardial thickness between the two scans.

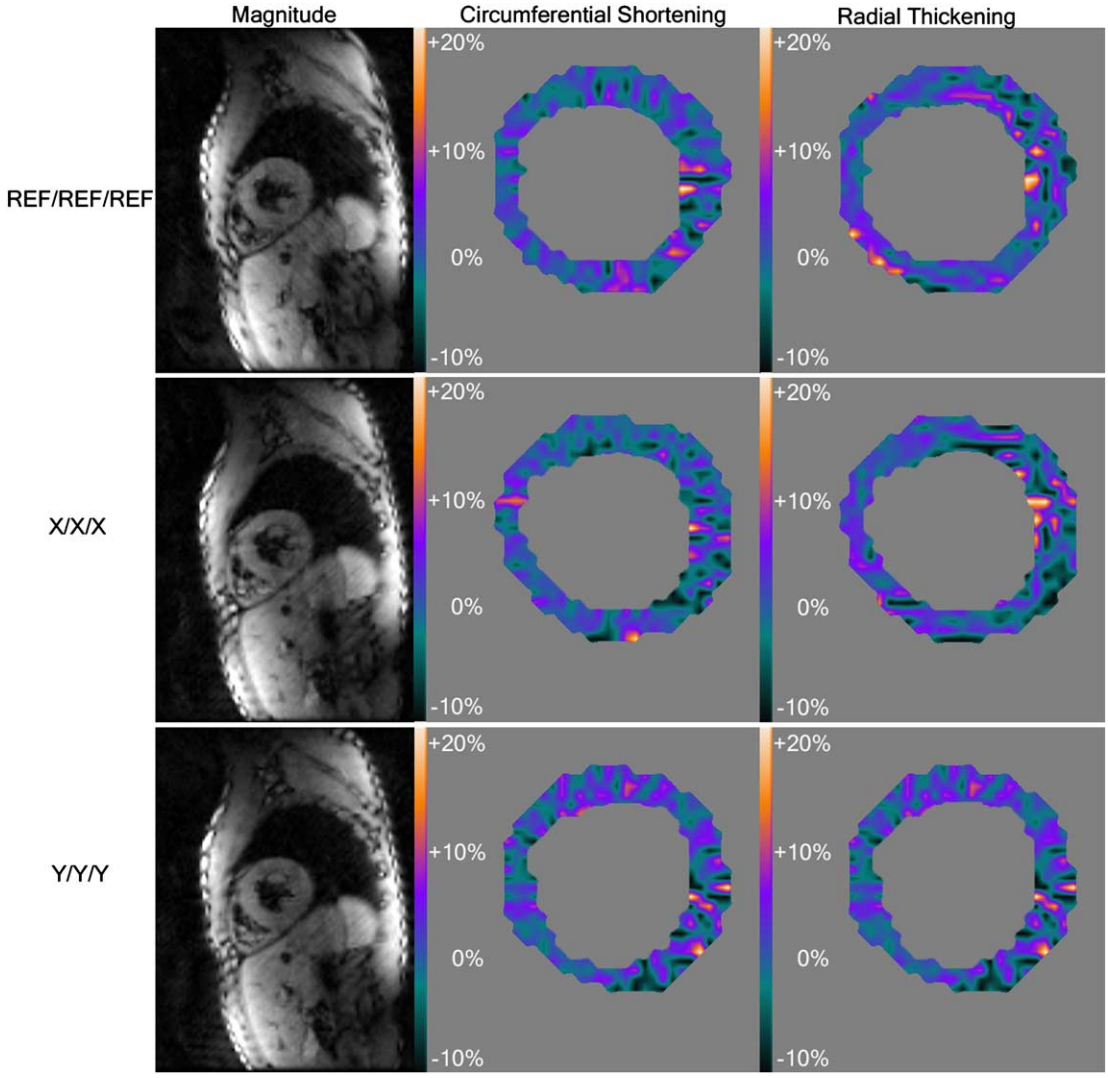

Fig. 3. SENSE-accelerated DENSE ($R = 2$) data from the normal volunteer of Fig. 2 demonstrate strain noise (all less than $1.6 \pm 5.1\%$ strain). These experiments were performed by repeating the same encoding gradient rather than acquiring both encoded and a reference scans. The top row corresponds to repeating the phase reference gradient waveform three times, the second row to repeating the X-encoded gradient waveform three times, and the last row to repeating the Y-encoded gradient waveform three times.

Table 1
Circumferential shortening (CS) and radial thickening (RT) noise strain measurements in vivo for the REF/REF/REF, X/X/X and, Y/Y/Y datasets for the normal volunteer scans ($n = 8$) (see Section 2)

	REF/REF/REF	X/X/X	Y/Y/Y
CS $R = 2$	0.1 ± 2.9	0.0 ± 3.3	0.1 ± 3.1
CS $R = 1$	0.5 ± 3.1	0.1 ± 2.9	-0.1 ± 3.0
RT $R = 2$	0.5 ± 4.2	0.2 ± 4.3	0.0 ± 3.5
RT $R = 1$	0.7 ± 4.1	0.4 ± 3.8	0.2 ± 3.9

All values are reported as mean percent strain $\pm$ SD. These results suggest that in vivo strain noise may be compounded by physiological parameters rather than the intrinsic noise of the DENSE experiment with or without SENSE acceleration ($R = 2$).

this slice of the heart. Note that in the core of the chronic infarct, the thinned out myocardium allows for partial volume particularly in radial thickening strain maps. Both SENSE-accelerated (top row) and conventional (bottom row) strain maps identify the corresponding inferior wall as an area of reduced deformation. However, the SENSE ($R = 2$) images were collected within 14 heartbeats rather than 26.

4. Discussion

SENSE can be used to accelerate phase maps. The current paper documents that high-quality maps of myocardial displacement can be derived from SENSE-accelerated DENSE. Feasibility is demonstrated in normal volunteers and a patient with a regional wall motion abnormality associated with a myocardial infarction.

This particular SENSE implementation, with a single non-encoded FSE low resolution B_1 map for reconstructing all three complex images (X/Y/REF) required

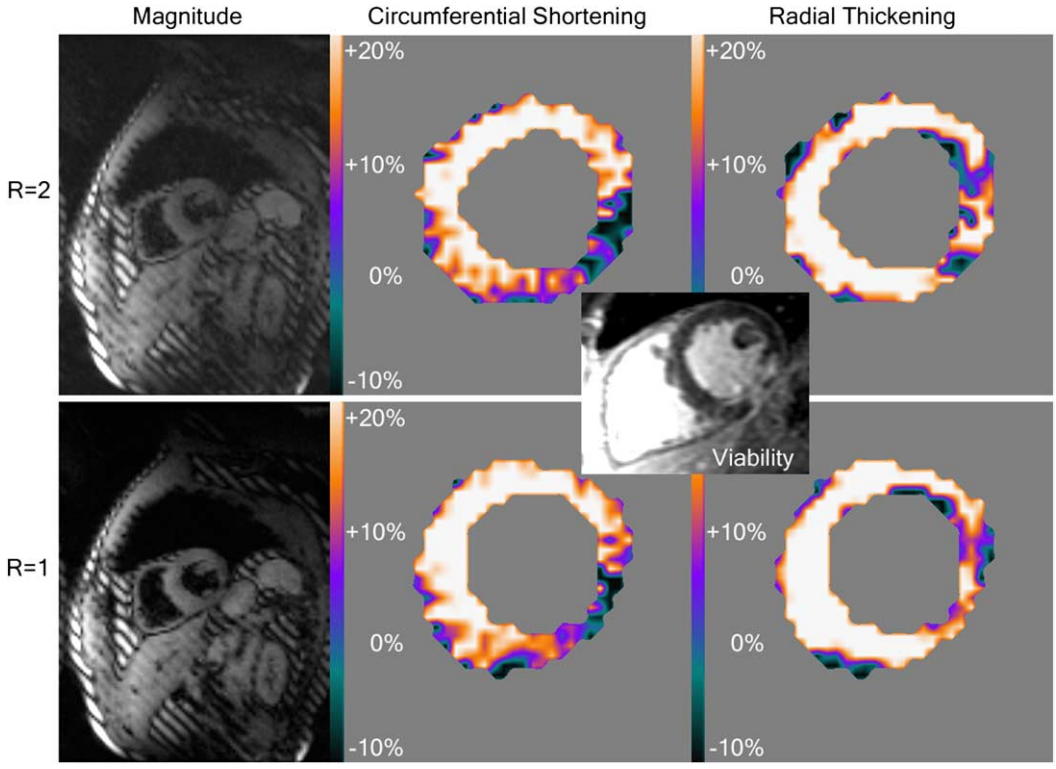

Fig. 4. Short axis strain maps from a patient with an inferior myocardial infarction show the applicability of SENSE rate 2 DENSE functional imaging within 14 heartbeats in a clinical setting. The top row shows circumferential shortening and radial thickening plots. Note the functional deficit in the inferior wall which corresponds to the region of the heart that exhibits delayed enhancement after gadolinium administration. For reference, data acquired from this highly cooperative patient with a 26 heartbeat breath-hold are shown in the bottom row.

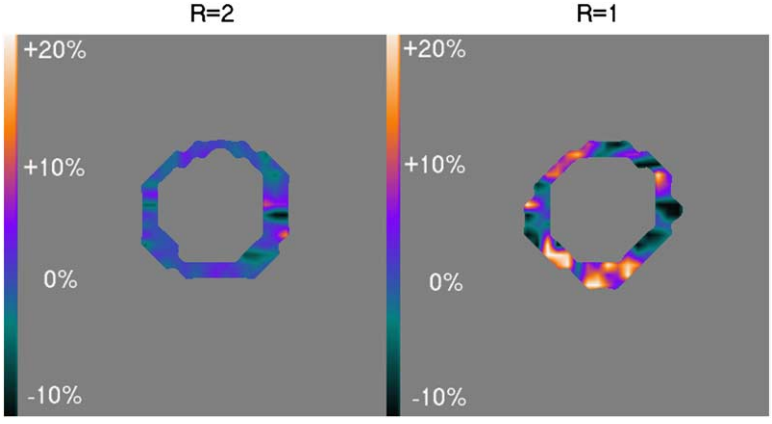

Fig. 5. Short axis strain maps from a volunteer demonstrate that strain noise with a 14 heartbeat acquisition ($R = 2$) appears lower than with a 26 heartbeat acquisition ($R = 1$). Patient motion observed during the prolonged breath-hold with $R = 1$ could account for this finding.

for 2D strain mapping, allows for better acceleration when compared to potentially collecting a separate map for each of the three DENSE images. The single FSE-based B_1 map provides an acceleration factor of $26/14 = 1.85$ vs $26/(14 + 3) = 1.53$ with separate maps. This is possible because the B_1 map acquisition seamlessly substitutes for the first of the two dummy scans required to set steady state prior to acquiring the desired dataset. Note that the steady state is dictated by the T_1 of the tissue and the interval bracketed by the end of the readout train (at end-systole) and the subsequent R-wave, i.e., it is not dependent on the formation (or not) of a stimulated echo. This is the result of locking the recovering magnetization about $z = 0$ due to the multiple refocusing RF pulses of the readout train [19]. The low resolution B_1 maps (128×24) can provide coil sensitivity information within one heartbeat. Since the coil spatial characteristics do not contain rapidly

changing components such an approximation is possible. The apodization of k-space along the phase direction was smoothened by the application of a Fermi filter prior to image reconstruction. Alternatively, higher resolution B_1 maps could potentially be acquired at the expense of acquisition time and acceleration.

Phantom experiments to evaluate phase noise indicate the random error in estimating phase increases with SENSE, as expected. However, the in vivo data do not appear limited by the intrinsic phase stability of the scanner but rather the noise has additional physiological components. We base this observation not only on the fact that the strain maps have substantially higher variability than the phase errors measured in the phantom but also on the observation that the SENSE acceleration did not increase the standard deviation of the strain estimates by at least a factor of $\sqrt{2}$. The summary results from the normal volunteer studies (Table 1) also show that the SENSE acceleration ($R = 2$) does not change the strain noise level when compared to the unaccelerated scans ($R = 1$) suggesting that thermal noise is not the limiting factor for DENSE, at least with this modest acceleration. Physiological strain noise due to patient or diaphragm motion can be overwhelming as seen in Fig. 5. Here, patient motion over the long 26 heartbeat breath-hold ($R = 1$) results in increased strain noise (as seen in the bright areas) when compared to the shorter SENSE-accelerated acquisition over 14 heartbeats ($R = 2$).

The desire to reduce the gradient moments of the motion encoding gradient pulses in DENSE for reduced intravoxel dephasing requires that the non-encoded FID and the stimulated anti-echo (STAE) be suppressed [5]. The FID can be suppressed either with an inversion pulse [8] or RF phase cycling [20], whereas the STAE can only be suppressed with phase cycling [4–6]. Therefore, the DENSE scans require multiple acquisitions that are added together prolonging the total breath-hold time to unacceptable levels for patient comfort. Implementing SENSE to accelerate DENSE scans was shown to provide strain maps of comparable quality to those reported earlier [1,5–9,21]. The strain noise level compared to non-accelerated DENSE (Table 1) remains low for the detection of functional hypokinesis (Fig. 4).

DENSE with RF phase-cycling [4] and SENSE acceleration [15] will allow for patient studies to take place within reasonable acquisition times without the need to segment the acquisition over separate breath holds. SPAMM myocardial tagging [3] has been used for some time in research scans and the most recent development of HARP phase-based processing methods [22] could potentially allow SPAMM to find utility in routine patient scans. Relative to tag-tracking methods, this reduction in data processing time by orders of magnitude with HARP becomes important for patient scans. However, such methods rely on isolating the first harmonic of the tagged image (a.k.a. the stimulated echo) from a k-space which also contains the 0th harmonic (a.k.a. FID) and the conjugate of the first harmonic (a.k.a. stimulated anti-echo) [19]. All three k-space components create the tagging pattern but two out of three are the source of artifacts [5] when phase-based methods are considered for tag tracking. Therefore, complex DENSE acquisitions [4–6], which rely on suppressing the two artifact-generating k-space components without introducing intravoxel dephasing signal losses, have a potential advantage in this regard.

The application of a very conservative acceleration rate of $R = 2$ was dictated mainly by the desire to speed up existing DENSE scans for patient studies. Higher acceleration factors could potentially allow DENSE to be acquired in even fewer heartbeats. However, such an application would require specially designed phased array coils for SENSE.

References

[1] A.H. Aletras, S. Ding, R.S. Balaban, H. Wen, DENSE: displacement encoding with stimulated echoes in cardiac functional MRI, J. Magn. Reson. 137 (1) (1999) 247–252.

[2] E.A. Zerhouni, Myocardial tagging by magnetic resonance imaging, Coron. Artery Dis. 4 (4) (1993) 334–339.

[3] L. Axel, L. Dougherty, MR imaging of motion with spatial modulation of magnetization, Radiology 171 (3) (1989) 841–845.

[4] A.H. Aletras, H. Wen, Methods and apparatus for mapping internal and bulk motion of an object with phase labeling in magnetic resonance imaging. International Application Published Under the Patent Cooperation Treaty 2001; WO 01/11380 A2:10/12/2001.

[5] A.H. Aletras, A.E. Arai, meta-DENSE complex acquisition for reduced intravoxel dephasing, J. Magn. Reson. 169 (2) (2004) 246–249.

[6] F.H. Epstein, W.D. Gilson, Displacement-encoded MRI of the heart using Cosine ANd Sine modulation to ELiminate artifact generating echoes, Proc. Int. Soc. Magn. Reson. Med. 11 (2003) 1566.

[7] A.H. Aletras, R.S. Balaban, H. Wen, High-resolution strain analysis of the human heart with fast-DENSE, J. Magn. Reson. 140 (1) (1999) 41–57.

[8] A.H. Aletras, H. Wen, Mixed echo train acquisition displacement encoding with stimulated echoes: an optimized DENSE method for in vivo functional imaging of the human heart, Magn. Reson. Med. 46 (3) (2001) 523–534.

[9] D. Kim, W.D. Gilson, C.M. Kramer, F.H. Epstein, Myocardial tissue tracking with two-dimensional cine displacement-encoded MR imaging: development and initial evaluation, Radiology 230 (3) (2004) 862–871.

[10] A. Haase, J. Frahm, D. Matthaei, W. Hanicke, H. Bomsdorf, D. Kunz, R. Tischler, MR imaging using stimulated echoes (STEAM), Radiology 160 (3) (1986) 787–790.

[11] J.M. Zhu, I.C. Smith, Stimulated anti-echo selection in spatially localized NMR spectroscopy, J. Magn. Reson. 136 (1) (1999) 1–5.

[12] R. Bammer, S.O. Schoenberg, Current concepts and advances in clinical parallel magnetic resonance imaging, Top. Magn. Reson. Imaging 15 (3) (2004) 129–158.

[13] D.K. Sodickson, W.J. Manning, Simultaneous acquisition of spatial harmonics (SMASH): fast imaging with radiofrequency coil arrays, Magn. Reson. Med. 38 (4) (1997) 591–603.

[14] M.A. Griswold, P.M. Jakob, R.M. Heidemann, M. Nittka, V. Jellus, J. Wang, B. Kiefer, A. Haase, Generalized autocalibrating partially parallel acquisitions (GRAPPA), Magn. Reson. Med. 47 (6) (2002) 1202–1210.
[15] K.P. Pruessmann, M. Weiger, M.B. Scheidegger, P. Boesiger, SENSE: sensitivity encoding for fast MRI, Magn. Reson. Med. 42 (5) (1999) 952–962.
[16] P. Kellman, F.H. Epstein, E.R. McVeigh, Adaptive sensitivity encoding incorporating temporal filtering (TSENSE), Magn. Reson. Med. 45 (5) (2001) 846–852.
[17] K.P. Pruessmann, M. Weiger, P. Boesiger, Sensitivity encoded cardiac MRI, J. Cardiovasc. Magn. Reson. 3 (1) (2001) 1–9.
[18] E. McVeigh, Regional myocardial function, Cardiol. Clin. 16 (2) (1998) 189–206.
[19] A.H. Aletras, R.Z. Freidlin, G. Navon, A.E. Arai, AIR-SPAMM: Alternative inversion recovery spatial modulation of magnetization for myocardial tagging, J. Magn. Reson. 166 (2) (2004) 236–245.
[20] S. Ryf, M.A. Spiegel, M. Gerber, P. Boesiger, Myocardial tagging with 3D-CSPAMM, J. Magn. Reson. Imaging 16 (3) (2002) 320–325.
[21] W.D. Gilson, Z. Yang, B.A. French, F.H. Epstein, Complementary displacement-encoded MRI for contrast-enhanced infarct detection and quantification of myocardial function in mice, Magn. Reson. Med. 51 (4) (2004) 744–752.
[22] N.F. Osman, W.S. Kerwin, E.R. McVeigh, J.L. Prince, Cardiac motion tracking using CINE harmonic phase (HARP) magnetic resonance imaging, Magn. Reson. Med. 42 (6) (1999) 1048–1060.